Investigation on the limit of weak infrared photodetection

Y. Yang, H. C. Liu,[a] M. R. Hao, and W. Z. Shen[a]
Key Laboratory of Artificial Structures and Quantum Control (Minister of Education), and Laboratory of Condensed Matter Spectroscopy and Optoelectronic Physics, Department of Physics, Shanghai Jiao Tong University, Shanghai 200240, China

(Received 4 August 2011; accepted 22 August 2011; published online 3 October 2011)

We investigate the limit of weak infrared photodetection based on a systematic analysis of three main noise mechanisms, and point out the principles to achieve the ultimate performance. Two key issues should be addressed to realize ultra-sensitive infrared photodetection: suppression of background radiation, selection and optimization of photodetectors. We quantitatively studied the dependence of ultimate performance on the background temperature and emissivity. It is revealed that the background limited infrared performance detectivity for mid-infrared photodetection can be increased from the range of 10^{10} to 10^{11} cmHz$^{1/2}$/W to 10^{15} cmHz$^{1/2}$/W or even higher values, when the background radiation temperature decreases from the ambient to liquid nitrogen temperature. Furthermore, we investigate the feasibility of photoconductive infrared photodetectors for ultra-sensitive photodetection. Our simulations shows that ideal quantum well infrared photodetectors (QWIPs) can reach background limited infrared performance at feasible operation temperatures facing even very weak background radiation. For specific and quantitative analyses, QWIPs are used as the examples. However, the conclusions apply to a broader range of cases. © *2011 American Institute of Physics*. [doi:10.1063/1.3642986]

I. INTRODUCTION

The first infrared photoconductive detector was invented in 1917.[1] Since 1930s, lead salt infrared photodetectors have been used for military applications.[2] Thereafter since 1950s, III-V (InSb, InGaAs, InAsSb), IV-VI (PbSnTe), and II-VI (HgCdTe) compound semiconductor materials have been investigated for infrared photodetectors.[3] These materials have tunable bandgap, high optical absorption coefficient and carrier mobility, as well as low thermal generation rate, making them suitable for infrared photodetection. Until now, the whole infrared spectrum from near-infrared to far-infrared has been covered by narrow gap infrared photodetectors. In addition, photodetectors based on intersubband transitions including quantum well infrared photodetectors (QWIPs)[4] and quantum dot infrared photodetectors have been developed.[5]

Piotrowski *et al.*[6] have studied the ultimate performance of infrared photodetectors. The optimal detectivity of a photoconductive detector is calculated to be about 1×10^{11} cmHz$^{1/2}$/W at 5 μm, and about 3×10^{10} cmHz$^{1/2}$/W at 10 μm, facing a 2π-solid-angle field of view (FOV) room temperature blackbody radiation, i.e., in the background limited infrared performance (BLIP) regime. The ultimate BLIP detectivity of photovoltaic detectors is higher than that for photoconductive detectors by a factor of square root of two. Today, these limitations have been closely approached. Mid-infrared photoconductive HgCdTe and photovoltaic InSb detectors working at liquid nitrogen temperature have detectivities higher than 1×10^{11} cmHz$^{1/2}$/W at 5 μm, and far-infrared PbSnTe photovoltaic detectors have detectivities of 2.5×10^{10} cmHz$^{1/2}$/W at 10 μm.[3] Meanwhile, intersubband infrared photodetectors with absorption efficiencies higher than 90% and detectivities comparable to interband infrared photodetectors have been demonstrated.[7] It should be highlighted that the mentioned detectivities are the ultimate performance limited by the background radiation instead of the detector property. Making even better photodetectors will not bring about a higher detectivity in the usual BLIP regime.

On the other hand, much higher infrared photodetection capability is called for. Infrared photodetection at ultra-low power densities of sub-picowatt or even single photon levels are useful for cutting-edge scientific exploration and quantum information. Single photon generation and detection in the visible and near-infrared region have been demonstrated using notably single photon avalanche diodes (SPADs) based on Si, InGaAs/InP SPADs,[8] superconducting transition-edge sensors,[9] and upconversion techniques.[10] In contrast, the capability in longer wavelength region is lagging far behind, partially due to the lack of ultra-high infrared photodetection techniques.

Two problems need to be addressed to realize ultra-sensitive infrared photodetection. First, background radiation should be suppressed so that high detectivity becomes possible. Facing room temperature background radiation, BLIP detectivity for mid-infrared photodetection is in the range of 10^{10} to 10^{11} cmHz$^{1/2}$/W. To further improve the detectivity, the background noise should be reduced. Ueda *et al.*[11] used an all-cryogenic spectrometer to create an ultra-low background radiation environment and got a high detectivity of 8×10^{14} cmHz$^{1/2}$/W at 15 μm. The spectrometer worked at liquid helium temperature. In this article, we quantitatively analyze the dependence of detectivity on background temperature and emissivity. Based on our calculations, BLIP

[a]Authors to whom correspondence should be addressed. Electronic addresses: h.c.liu@sjtu.edu.cn and wzshen@sjtu.edu.cn.

detectivity in the order of 10^{15} cmHz$^{1/2}$/W can be expected for the mid-infrared range, using a liquid nitrogen low-emissivity all-cryogenic spectrometer, in combination with an optimized infrared photodetector.

Second, infrared photodetectors should be optimized to minimize the noise and effectively collect the signal. For mid-infrared and far-infrared regions, charge-sensitive infrared phototransistors[11] and hot-electron nanobolometers[12] have demonstrated the capability for ultra-sensitive detection. In this article, we investigate the feasibility of using photoconductive infrared photodetectors, the mainstream infrared photodetection devices, for this purpose. For specific and quantitative analyses, we use QWIPs as the example case though the conclusions apply to a broader range of infrared photodetectors. It is revealed that narrowband infrared photodetectors are advantageous to achieve ultimate performance at specified wavelength or within a narrow wavelength band. Our calculations show that QWIPs are able to reach BLIP condition at feasible operation temperatures facing even very weak background radiation.

II. THEORETICAL BACKGROUND

In general, infrared photodetector noises have three sources, (a) device noise, (b) background noise, and (c) signal noise. The device noise is the current noise in the absence of illumination. The background noise is produced by the background radiation incident on the photodetector, and the signal noise is caused by the incident signal light. More specifically, device noises can be categorized into three types: Johnson noise, generation-recombination (g-r) noise, and $1/f$ noise. For infrared photoconductive detector working at optimal conditions, Johnson noise and $1/f$ noise seldom limit the detector performance. The main source of device noise is the g-r noise, which is caused statistically by the fluctuation of thermal generation and recombination of carriers. The device noise caused by g-r is expressed as[13]

$$i_{\mathrm{n,Device}} = \sqrt{4egi_{\mathrm{dark}}\Delta f}, \tag{1}$$

where e is the electron charge, g is the current gain, i_{dark} is the dark current, and Δf is the measurement bandwidth.

Infrared photodetectors are illuminated with background radiations, which are normally assumed as a gray body radiation. The incidence of photons on the photodetector is a homogeneous Poisson process. The lifetime of photoexcited carriers in a photoconductive detector also obeys a Poisson distribution. For a photoconductive photodetector, the noise resulted from background radiation is[13]

$$i_{\mathrm{n,BB}} = \sqrt{4egi_{\mathrm{BB}}\Delta f}, \tag{2}$$

where i_{BB} is the photocurrent induced by the background radiation. Similarly, input signal light results in a signal noise $i_{\mathrm{n,Signal}}$[13]

$$i_{\mathrm{n,signal}} = \sqrt{4egi_{\mathrm{Signal}}\Delta f}, \tag{3}$$

where i_{Signal} is the photocurrent induced by the signal light. Compared with the background noise and device noise, the signal noise is negligible for normal applications. The total noise i_{n} of a photoconductor satisfies:

$$i_{\mathrm{n}}^{\ 2} = i_{\mathrm{n,BB}}^{\ 2} + i_{\mathrm{n,Signal}}^{\ 2} + i_{\mathrm{n,Device}}^{\ 2}. \tag{4}$$

These three noise sources compete with each other. Practically, one of them will dominate over the others, depending on the operation conditions. In the following, we discuss the approaches to achieve high infrared performance.

We analyze in Sec. III A the dependence of device performance on operation temperature. The detectivity can be substantially improved by cooling the photodetector, but it will saturate when the operation temperature is below the BLIP temperature. The only choice to further improve the detectivity is to reduce the background noise. In Sec. III B, we investigate three aspects to suppress the background noise: the absorption spectrum, the temperature, and the emissivity of background radiation. In Sec. III C, we examine the influence of signal noise on infrared photodetector performance. Although signal noise can be ignored for most common applications, it should be considered when the background noise and device noise are suppressed to very low levels.

III. RESULTS AND DISCUSSION

A. Device noise

An effective way to improve infrared photodetector detectivity is to cool the device. The device noise can be substantially suppressed via reducing the operation temperature, since the dark current of a semiconductor photodetector, either interband or intersubband, decreases rapidly with deceasing operation temperature.

To be specific, we use a typical QWIP (Sample S2 in Ref. 14, referred to as S2 hereafter) to carry out the following analyses. The QWIP active region is composed of 100 repeats of GaAs (54 Å thick)/$Al_{0.24}Ga_{0.76}As$ (300 Å thick) layers. The quantum well center is doped with Si to a density of 4×10^{11} cm^{-2}, and the structure parameters are properly chosen to meet the bound-to-quasibound configuration. The absorption spectrum of a QWIP can be approximated by a Lorentz line shape centered at a peak wavelength λ_{p} with a linewidth λ_{half}, within the wavelength range around the peak wavelength. For calculations in this paper, the integration range is from λ_{p}-$2\lambda_{\mathrm{half}}$ to $\lambda_{\mathrm{p}}+2\lambda_{\mathrm{half}}$. QWIP S2 has an absorption efficiency of 0.4% per quantum well at the peak wavelength of 9 μm, and the absorption linewidth is about 1 μm. The excited carrier lifetime is 11.8 ps. The BLIP temperature is measured to be 72 K, facing 90° FOV 300 K background radiation.

According to the three-dimensional carrier drift model of QWIPs, the dark current is proportional to the density of carriers excited above the barrier:[13]

$$i_{\mathrm{dark}} = evA\left(\frac{m_{\mathrm{b}}k_{\mathrm{B}}T_{\mathrm{op}}}{2\pi\hbar^2}\right)^{3/2}\exp\left(-\frac{\Delta E}{k_{\mathrm{B}}T_{\mathrm{op}}}\right), \tag{5}$$

here v is the carrier drift velocity under device bias, A is the device area, T_{op} is the device operation temperature, m_{b} is

the carrier effective mass in the barrier, and ΔE is the barrier height referenced the Fermi level. For an 8 to 12 μm QWIP, the typical value of ΔE is 120 meV.[13] In Eq. (5), only the drift of thermally excited carriers is taken into account, while the tunneling current is ignored. The dark current of QWIPs has three causes, drift of thermally excited carriers, inter-well tunneling, and defect-assisted tunneling. For relatively high operation temperatures, the first factor has been experimentally confirmed to be the main source, and the latter two factors can be ignored. For low operation temperatures, the latter two factors start to play a role. However, the inter-well tunneling and defect-assisted tunneling can be completely suppressed by using sufficiently wide barriers with low defect densities. The goal of present paper is to investigate the ultimate infrared photodetection performance and the feasibility of using QWIPs for this purpose, so we consider an ideal QWIP which is specifically designed and properly fabricated. Therefore, only the drift of thermally excited carriers is taken into account.

The validity of Eq. (5) has been experimentally verified for operation temperatures ranged from 60 to 85 K.[14] The dark current of QWIP S2 is measured to be 6.0×10^{-7}, 1.4×10^{-5}, and 4.5×10^{-4} A/cm^2 for operation temperatures of 60, 72, and 85 K, respectively, under 2 V device bias. In this paper, we use Eq. (5) to calculate the dark current at all operation temperatures, ignoring the tunneling component. The parameters for calculation in are $m_b = 0.094 m_e$, with m_e the electron mass, and$\Delta E = 120$ meV.

Figure 1(a) shows the dependence of noises on the operation temperature of QWIP S2 under 90° FOV room temperature blackbody radiation, ignoring the signal noise. The dark current noise is calculated using Eq. (1) and Eq. (5), while the background noise is calculated using Eq. (2) and the expression for background current. During the calculation, we assume the measurement bandwidth Δf to be 10^4 Hz, and employ a current gain of 0.1 (experimental value). These values are also used for noise current calculation in the following contexts. The curves of background noise and device noise intersect at the BLIP temperature, 72 K. At operation temperatures higher than the BLIP temperature, the device noise dominates. Cooling the sample will effectively reduce the device noise, and thus the total noise level. At operation temperatures below the BLIP temperature, the background noise becomes the main noise source. Figure 1(b) shows the temperature dependent detectivity. The detectivity is only 1.2×10^7 cmHz$^{1/2}$/W at 300 K operation temperature. It increases drastically to 3.8×10^{10} cmHz$^{1/2}$/W when the device works under BLIP condition. To achieve even higher detectivities, the background noise must be reduced.

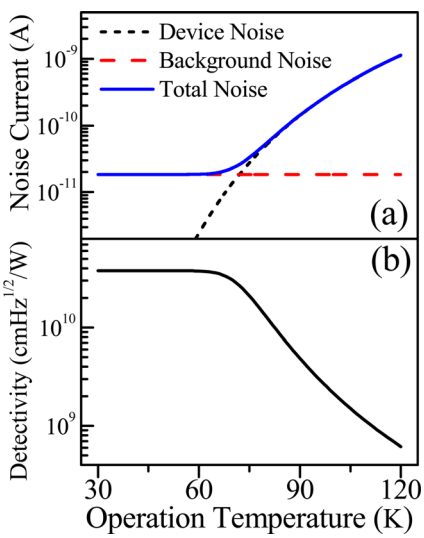

FIG. 1. (Color online) Dependence of (a) noises and (b) detectivity of QWIP S2 on the operation temperature. The photodetector faces 90° FOV 300 K background radiation.

B. Background noise

Assuming an infrared photodetector looking at a background radiation from 90° FOV, the incident radiation power $P(\lambda)\mathrm{d}\lambda$ within the wavelength interval $\mathrm{d}\lambda$ at wavelength λ is

$$P(\lambda)d\lambda = \varepsilon \frac{\pi hc^2}{\lambda^5} \frac{Ad\lambda}{\exp(hc/k_B T_{BB}\lambda) - 1}, \tag{6}$$

where ε is the emissivity, h is the Planck constant, c is the speed of light in vacuum, and T_{BB} is the background temperature in Kelvins. The emissivity of an ideal blackbody is unity. Real objects are normally treated as gray bodies, which have constant emissivities less than one.

The photocurrent i_{BB} induced by the background radiation is

$$i_{BB} = \int \frac{eg\eta(\lambda)P(\lambda)\lambda}{hc} d\lambda. \tag{7}$$

For a photodetector working under BLIP condition, the device noise and signal noise can be ignored. Using these definitions, we get the background limited specified detectivity at wavelength λ:

$$D^*_{BL}(\lambda) = \frac{\lambda\eta(\lambda)}{hc} \left(\int \varepsilon\eta(\lambda) \frac{4\pi c}{\lambda^4} \frac{1}{\exp(hc/k_B T_{BB}\lambda) - 1} d\lambda \right)^{-1/2}. \tag{8}$$

For a specified wavelength λ, the BLIP detectivity $D^*_{BL}(\lambda)$ is determined by three parameters: the absorption spectrum $\eta(\lambda)$, the temperature of background radiation T_{BB}, and the emissivity ε of the background.

1. Background radiation temperature and emissivity

The total radiation power of a blackbody source is proportional to $T_{BB}{}^4$. The background radiation power at 77 K on a photodetector is only four thousandths of the radiation power at 300 K. Taking into account of the absorption spectrum, the absorbed radiation by an infrared photodetector can be reduced more significantly. As an example, Fig. 2(a) shows the dependence of noises on the background temperature calculated from Eqs. (2) and (7), with an operation temperature of 60 K. When the background temperature is reduced from 300 to 77 K, the background radiation absorbed by the photodetector is decreased by more than 10^4

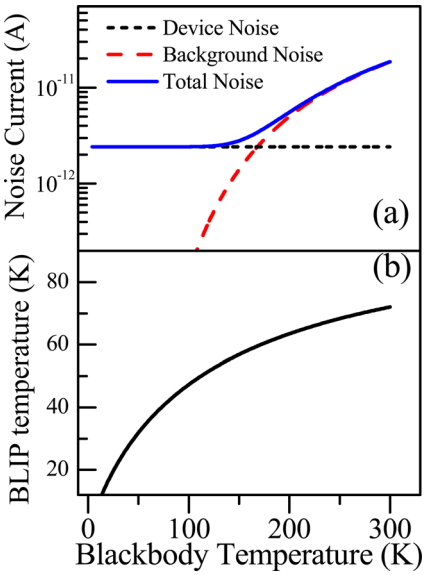

FIG. 2. (Color online) Dependence of (a) noises with 60 K operation temperature, and (b) BLIP temperature on background radiation temperature for QWIP S2.

times, and the background noise [red dashed curve in Fig. 2(a)] is therefore reduced by 100 times.

Figure 2(a) shows that the background noise equals to the device noise at 150 K background temperature under 60 K operation temperature. In other word, the BLIP temperature is 60 K facing 150 K background temperature. Obviously, the BLIP temperature decreases with the decreasing background radiation temperature [Fig. 2(b)], since the total background radiation is going down. The BLIP temperatures are 72, 41, and 4 K, respectively, at background temperatures of 300 K (room temperature), 77 K (liquid nitrogen temperature), and 4.2 K (liquid helium temperature).

Figure 3 shows the peak detectivity of QWIP S2 as a function of the detector temperature and the background temperature. Some points worth noting are as follows.

1. The peak detectivity is 1.2×10^7 cmHz$^{1/2}$/W at 300 K background temperature and 300 K detector temperature where it is limited by device noise. By cooling the photodetector to 77 K, a detectivity of 3.8×10^{10} cmHz$^{1/2}$/W is reached. Thus, infrared photodetectors generally work at cryogenic temperatures.
2. A much higher BLIP detectivity of 5.1×10^{13} cmHz$^{1/2}$/W is obtained for 77 K background temperature, about 133 times increase from the BLIP detectivity for 300 K background temperature. Assuming the area of the photodetector to be 1 mm^2, the sampling rate to be 10 kHz, the noise equivalent power is calculated to be 2.0×10^{-13} W-sub-picowatt level. To achieve this performance level, all parts of the measurement setup should be cooled to liquid nitrogen temperature, and there should be a cold shield to screen the outside background radiation.
3. Facing 40 K blackbody radiation as the background, the BLIP detectivity is 2.2×10^{17} cmHz$^{1/2}$/W. Using the same photodetector and measurement parameters as in above paragraph, the noise equivalent power under BLIP condition is calculated to be 4.5×10^{-17} W, which corresponds to a 9 μm noise photon flux of about 2000 Hz. The single photon level detection therefore would be possible. The challenge is how to reach BLIP condition facing such weak background radiation.

Based on our calculations, the BLIP temperature is 28 K for QWIP S2, facing 40 K background radiation. We arrive at this result under the assumption that the QWIP dark current satisfies Eq. (5), and the *g-r* noise to be the main device noise. For operation temperatures higher than 50 K, these assumptions have been verified.[14] However, the validity of these assumptions under low operation temperatures still needs to be investigated.

Equation (8) indicates that the emissivity ε of background radiation matters as well. The background radiation power is proportional to the emissivity. Therefore, the detectivity at a specified wavelength is inversely proportional to $\sqrt{\varepsilon}$. To take advantage of this, we suggest that all surfaces seen by the infrared photodetector during measurement should be covered by layers with low emissivity, e.g., polished gold with an emissivity of about 0.01. The detectivity can be improved by another order of magnitude.

In above discussions, we use the performance at 9 μm wavelength as an example. The performance at other wavelengths has similar behaviors, yet there are some numerical differences. Figure 4 shows the wavelength dependent BLIP

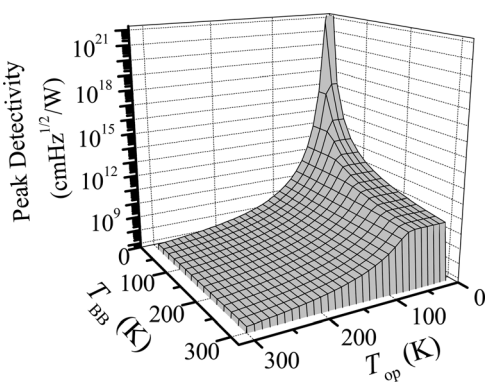

FIG. 3. Dependence of peak detectivity on the blackbody radiation temperature T_{BB} and operation temperature T_{op} for QWIP S2.

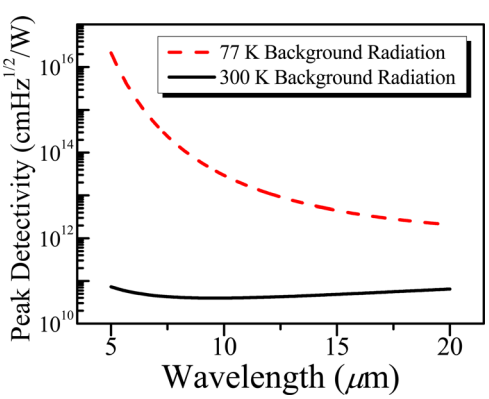

FIG. 4. (Color online) Wavelength dependent BLIP peak detectivity for a series of QWIPs, facing 300 K and 77 K background radiation, respectively.

peak detectivity for a series of QWIPs, facing 300 K and 77 K background radiation, respectively. For each QWIP, the ratio of absorption linewidth to peak wavelength is 0.1. For all wavelengths, the peak detectivity is obviously increased by reducing the background temperature from 300 K to 77 K. However, the amount of increase is different: it is about 3×10^5 times at 5 μm, more than 140 times at 9 μm, and about 30 times at 20 μm.

2. Absorption spectrum

In our previous paper,[14] we have investigated a series of QWIPs with different doping concentrations in the quantum wells. The samples have different absorption values but nearly the same absorption spectrum line shape. The BLIP detectivity relates to the absorption quantum efficiency by

$$D^*_{\mathrm{BL}}(\lambda) \propto \sqrt{\eta(\lambda)}. \tag{9}$$

This conclusion is not only valid for QWIPs, but also for other photoconductive infrared photodetectors. Equation (9) can be easily deduced from Eq. (8). The logic is straightforward: to have high detectivity at a wavelength λ, high absorption efficiency at this wavelength is desired so that more signal radiation can be detected.

Equation (8) indicates that the detectivity $D^*_{\mathrm{BL}}(\lambda)$ is not just determined by the absorption at the targeted wavelength, but also affected by the absorption at other wavelengths, in other word, the absorption spectrum line shape. The linewidth of QWIPs is associated with the excited carrier lifetime and interface roughness, which can be tuned to some degree. For a QWIP with a fixed number of period and doping, the integrated absorption efficiency is constant. The peak absorption rate decreases when the absorption linewidth increases [Fig. 5(a)]. Figure 5(b) shows dependence of BLIP peak detectivity $D^*_{\mathrm{BL}}(\lambda)$ on the linewidth of a series of QWIPs peaked at 9 μm, facing 77 K blackbody radiation with an emissivity of 0.01 from 90° FOV. The peak detectivity is 1.4×10^{15} cmHz$^{1/2}$/W for 0.5 μm linewidth, and 1.2×10^{14} cmHz$^{1/2}$/W for 2 μm linewidth.

Above analysis shows that a narrowband infrared photodetector is superior, if the ultimate goal is to have high detectivity at a specified wavelength or within a narrow wavelength band. The benefit of narrower response range is twofold. First, the peak absorption rate increases, so the responsivity becomes higher. Second, a smaller portion of the background radiation is seen, and the background noise would be lower. Therefore, narrowband infrared photodetectors can also be useful for applications such free space communication and trace gas detection, since the interference (not only blackbody radiation) from other wavelengths is suppressed.

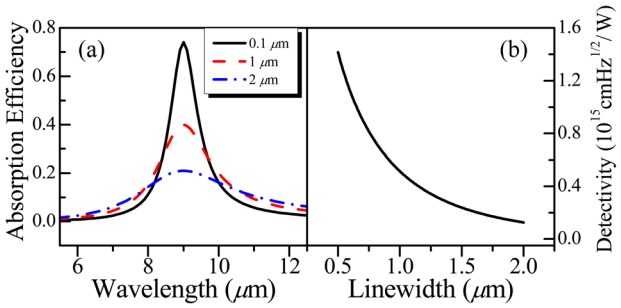

FIG. 5. (Color online) (a) Absorption spectra of a series of QWIPs with different linewidths, and (b) dependence of the peak detectivity and broadband detectivity on the linewidth of a series of QWIPs peaked at 9 μm under the BLIP condition. The detectors face 77 K backzground radiation with an emissivity of 0.01 from 90° FOV.

In above discussions, we focus on the detectivity at a specified wavelength or within a narrow wavelength band. In other application such as infrared imaging, the signal light to be detected is broadband. Accordingly, what matters is the broadband detectivity which describes a photodetector's performance over a wide wavelength range. Broadband infrared photodetectors can provide higher detectivities and therefore they are better choices. The other advantage of broadband photodetectors is that a wide wavelength range can be covered with one broadband infrared photodetector. For example, it takes only one HgCdTe photodetector to cover the wavelength range between 3 to 12 μm, while several QWIPs have to be used for the same wavelength range.

C. Signal noise

We have shown that the background noise and device noise can be suppressed to allow infrared photodetection at ultra-low levels. In such cases, the signal noise can become the major noise mechanism, and we reach the signal noise limited regime, the ideal operation situation for infrared detection. Using the definitions, we get the signal noise:

$$i_{\mathrm{n,Signal}} = 2eg\sqrt{\frac{\eta(\lambda)\lambda\Delta f}{hc}P_{\mathrm{Signal}}A}, \tag{10}$$

where P_{Signal} is the signal power density.

Figure 6(a) shows the dependence of noises on the background radiation temperature, for QWIP S2 facing 9 μm signal with a power density of 1×10^{-12} W/cm^2. For a 1 mm^2 area device, this corresponds to a signal flux of 4.5×10^5 photons per second. The black short dashed curve is the background noise, the red dashed curve is the signal noise and the blue solid one is total noise. The operation temperature is set low (e.g., 4.2 K) so that the device noise is negligible. The background noise and signal noise become equal at

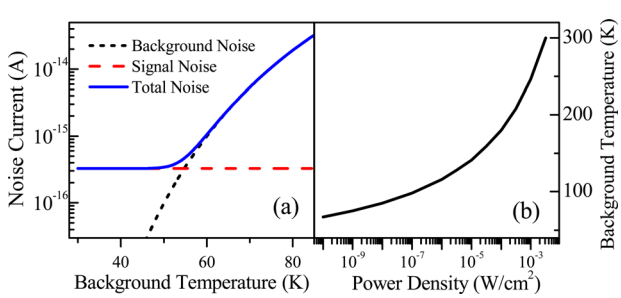

FIG. 6. (Color online) (a) Dependence of noises on the background radiation temperature, for QWIP S2 with an operation temperature of 4.2 K and a signal power density of 1×10^{-12} W/cm^2, (b) the background radiation temperature equalizing background noise with signal noise.

a background radiation temperature of 54 K. Here we call it the signal noise limited background temperature (SLBT). Background noise dominates at background temperatures higher than SLBT, and signal noise becomes the main noise mechanism at lower background temperatures. Figure 6(b) shows the SLBT as a function of signal power density. Obviously, the signal noise limited situation is easier to achieve at higher signal power densities: the SLBT is 300 K at a signal power density of 3.2 mW/cm^2, and 67 K at a signal power density of 1×10^{-10} W/cm^2.

IV. CONCLUSION

In summary, we have investigated the limit of weak infrared photodetection, and point out the principles to achieve the ultimate performance. Three main noise sources, device noise, background noise, and signal noise, compete with each other, and one of them will dominate over the others depending on the operation situation. Facing room temperature background radiation, the ultimate detectivity limited by the background noise is in the range of 10^{10} to 10^{11} $cmHz^{1/2}/W$. We show that background noise decrease rapidly when the background radiation temperature is cooled from room temperature to 77 K or even lower temperatures. Accordingly, the BLIP detectivity can be improved to 10^{15} $cmHz^{1/2}/W$ or even higher values. Single photon level infrared photodetection is also feasible under specified conditions. In addition, we point out the principles of device selection and optimization to achieve the ultimate performance: a narrowband infrared photodetector is preferred to achieve ultimate detectivity at a specified wavelength or within a narrow wavelength range, while a broadband photodetector is a better choice for most other applications. Our simulations show that QWIPs are able to reach BLIP condition at feasible operation temperatures facing even very weak background radiation.

ACKNOWLEDGMENTS

This work was supported in part by the National Major Basic Research Projects (2011CB925603 and 2012CB934302), Natural Science Foundation of China (10734020 and 11074169), and Shanghai Municipal Major Basic Research Project (09DJ1400102).

[1]T. W. Case, Phys. Rev. **9**, 305 (1917).
[2]R. J. Cushman, Proc. IRE **47**, 1471 (1959).
[3]A. Rogalski, Prog. Quant. Electron. **27**, 59 (2003).
[4]B. F. Levine, J. Appl. Phys. **74**, R1 (1993).
[5]S. A. McDonald, G. Konstantatos, S. G. Zhang, P. W. Cyr, E. J. D. Klem, L. Levina, and E. H. Sargent, Nat. Mater. **4**, 138 (2005).
[6]J. Piotrowski and W. Gawron, Infrared Phys. Technol. **38**, 63 (1997).
[7]A. Rogalski, Rep. Prog. Phys. **18**, 2267 (2005).
[8]P. A. Hiskett, G. S. Buller, A. Y. Loudon, J. M. Smith, I. Gontijo, A. C. Walker, P. D. Townsend, and M. J. Robertson, Appl. Opt. **39**, 6818 (2000).
[9]A. E. Lita, A. J. Miller, and S. W. Nam, Opt. Express **16**, 3032 (2008).
[10]M. A. Albota and F. N. C. Wong, Opt. Lett. **29**, 1449 (2004).
[11]T. Ueda and S. Komiyama, Sensors **10**, 8411 (2010).
[12]B. S. Karasik, S. V. Pereverzev, D. Olaya, M. E. Gershenson, R. Cantor, J. H. Kawamura, P K. Day, B. Bumble, H. G. LeDuc, S. P. Monacos, D. G. Harding, D. Santavicca, F. Carter, and D. E. Prober, SPIE Proc. **7741**, 774119 (2010).
[13]H. Schneider and H. C. Liu, *Quantum Well Infrared Photodetectors—Physics and Applications* (Springer, Berlin, 2007).
[14]Y. Yang, H. C. Liu, W. Z. Shen, N. Li, W. Lu, Z. R. Wasilewski, and M. Buchanan, IEEE J. Quant. Electron. **45**, 623 (2009).